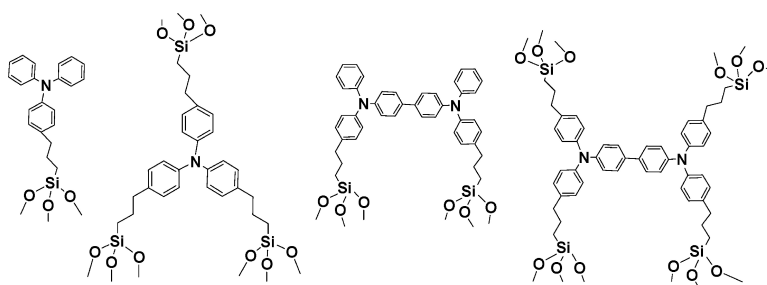


Molecularly “Engineered” Anode Adsorbates for Probing OLED Interfacial Structure–Charge Injection/Luminance Relationships: Large, Structure-Dependent Effects

Qinglan Huang, Guennadi Evmenenko, Pulak Dutta, and Tobin J. Marks

J. Am. Chem. Soc., **2003**, 125 (48), 14704-14705 • DOI: 10.1021/ja037174b • Publication Date (Web): 08 November 2003

Downloaded from <http://pubs.acs.org> on March 30, 2009



More About This Article

Additional resources and features associated with this article are available within the HTML version:

- Supporting Information
- Links to the 5 articles that cite this article, as of the time of this article download
- Access to high resolution figures
- Links to articles and content related to this article
- Copyright permission to reproduce figures and/or text from this article

[View the Full Text HTML](#)

Molecularly “Engineered” Anode Adsorbates for Probing OLED Interfacial Structure–Charge Injection/Luminance Relationships: Large, Structure-Dependent Effects

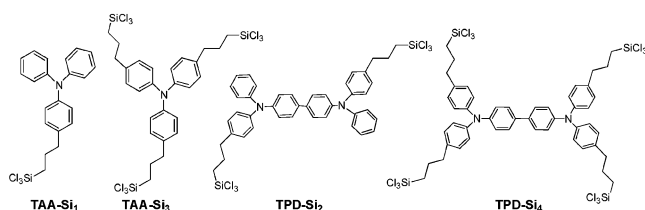
Qinglan Huang, Guennadi Evmenenko, Pulak Dutta, and Tobin J. Marks*

Department of Chemistry and the Materials Research Center, Northwestern University,
Evanston, Illinois 60208-3113

Received July 9, 2003; E-mail: t-marks@northwestern.edu

Research on organic solid-state electroluminescence has burgeoned with the advent of practical and near-practical polymer and small-molecule organic light-emitting diodes (OLEDs).¹ The synthesis and implementation of new bulk charge transporting and emissive materials has afforded much fundamental information and has resulted in greatly enhanced quantum efficiency, brightness, and stability. Nevertheless, nanoscale interfacial phenomena which are inextricably connected with charge injection,² energy level matching,³ physical decohesion and delamination,⁴ anode corrosion and ion injection,⁵ interface dipoles,⁶ image forces,⁷ and exciton quenching⁸ are poorly understood, and their precise control is of great importance if electroluminescent response and durability are to be truly optimized. We report here the implementation of a series of probe molecules having incrementally varied structures and surface linking characteristics, designed to form conformal, robust, self-assembled monolayers^{2a,9} on OLED ITO anodes. It is seen that molecular structure effects on OLED charge injection and response characteristics can be very large.

The chlorosilane-tethered series shown below was synthesized



and purified under rigorously anhydrous and anaerobic conditions.¹⁰ Self-limited anaerobic chemisorption of these compounds onto smooth (~2.5 nm RMS roughness), plasma-cleaned ITO surfaces was carried out by immersing ITO substrates in 1.0 mM toluene solutions,¹⁰ followed by rinsing, drying and curing. Adsorbate characterization included AFM, aqueous contact angles, optical spectroscopy, cyclic voltammetry, XPS, UPS, and X-ray reflectivity (XRR), revealing formation of conformal, largely pinhole-free self-assembled monolayers (SAMs) with sub-nanometer thickness control and essentially identical aggregate surface energies, ionization potentials, and coverages (Table 1).

The effect of SAM structure on ITO–organic interfacial hole injection was first investigated by fabricating hole-only devices¹¹ (Figure 1). Since the only difference in the four types of devices is in SAM molecular structure, the results clearly reveal a significant structure sensitivity of hole injection across the nano interfacial region. For example, hole current densities at 25 V are ~0.0004 A/cm² (TAA-Si₃) < ~0.004 A/cm² (TAA-Si₁) < ~0.01 A/cm² (TPD-Si₂) < ~0.04 A/cm² (TPD-Si₄); hole injection fluences vary by 1 to 2 orders of magnitude. The current densities are somewhat lower than those in OLEDs studied below, principally due to the

Table 1. Characteristics of Anode Functionalization Layers^a

	TAA-Si ₁	TAA-Si ₃	TPD-Si ₂	TPD-Si ₄
λ_{max} (nm)	303	304	352	352
thickness (nm) ^b	1.2	1.4	1.8	1.6 ^c
RMS roughness (nm) ^b	0.4	0.7	0.7	1.3
aq contact angle (deg)	90	87	90	90
$E_{\text{p,a}}/E_{\text{p,c}}$ (V) ^d	1.180/ 0.798	1.200/ 0.734	1.160/ 0.815	1.130/ 0.799
coverage Γ ($\times 10^{-10}$ mol/cm ²) ^e	4.5	4.2	2.5 ^f	2.1 ^f
$\Delta E_{\text{p,1/2}}$ (mV) ^g	340	460	350	440
IP (eV) ^h		5.8	6.1	

^a Experimental details in Supporting Information. ^b From X-ray reflectivity of samples identically deposited on oxide-coated (111)Si. ^c This parameter is uncertain due to surface roughness. ^d From cyclic voltammetry (10 V/s). ^e Estimated by CV (0.1 V/s). ^f CV coverage consistent with XRR data assuming two-electron process. ^g 0.1 V/s scan rate. $\Delta E_{\text{p,1/2}} > 90.6$ mV, indicating redox site interactions, site heterogeneity, or both. ^h From UPS.

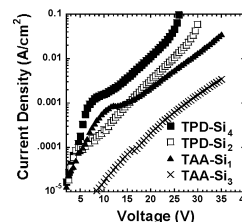


Figure 1. Effect of SAM structure on hole injection for hole-only devices having structures ITO/SAM/*N,N*-naphthalyl-*N,N'*-phenyl-biphenyl-4,4'-diamine (NPB, 400 nm)/Au/Al.

thicker HTL (hole transport layer) deposited in the hole-only devices. OLEDs were next fabricated to examine SAM structure effects on EL response, which are also significant. Bare ITO and phenylsilane SAM-coated ITO-based devices were also fabricated for comparison. In Al cathode OLEDs, luminances at 20 mA/cm² (a standard current density for device evaluation) are 200 cd/m² (TPD-Si₄) < 230 cd/m² (TPD-Si₂) < 400 cd/m² (TAA-Si₁) < 570 cd/m² (TAA-Si₃) (Figure 2). This order of current efficiency is *opposite* to that of the hole current densities measured above and can be understood in terms of electron injection-limited electron–hole recombination events.¹² Appreciable forward external quantum efficiency (η_{ext}) variations evidence large, anode–organic interface effects on OLED charge recombination, currently an imprecisely understood process.¹³ Compared to bare ITO-based devices, SAM-induced OLED performance enhancement is observed, with the modest phenylsilane SAM improvement mainly attributable to improved ITO anode–HTL contact via surface energy matching.¹⁴ Comparison between phenyl and triarylamine silane SAMs indicates that the latter result in lower anode–HTL hole injection barriers, agreeing with lower turn-on and operating voltages at identical

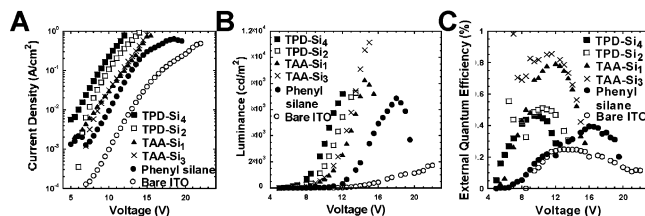


Figure 2. Responses of OLEDs having structures ITO/(SAM)/NPB/tris-(8-hydroxyquinolato)aluminum (AlQ): 1% diisoamylquinacridone (DIQA)/Al. (A) Current density vs. voltage. (B) Luminance vs. voltage. (C) η_{ext} vs. voltage.

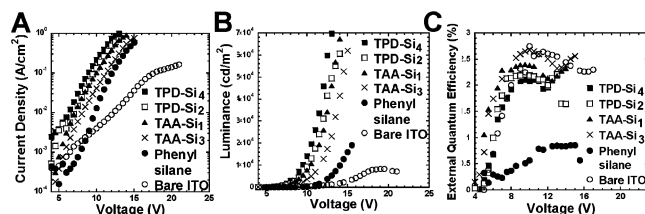


Figure 3. Responses of OLEDs having structures ITO/(SAM)/NPB/AIQ: 1% DIQA/2,9-dimethyl-4,7-diphenyl-1,10-phenanthroline (BCP)/Li/AgMg. (A) Current density vs. voltage. (B) Luminance vs. voltage. (C) η_{ext} vs. voltage.

luminance. In a second device configuration with enhanced electron injection and a hole-blocking layer (Figure 3),¹⁵ the hole–electron density imbalance is substantially alleviated, and more efficient recombination is expected. This is indeed observed, with the maximum luminance and η_{ext} achieved by **TPD-Si₄**-based OLEDs ($\sim 70\,000$ cd/m² and 2.1%, respectively) nearly 1 order of magnitude and 5 times greater, respectively, than in Figure 2. Note again the poorer response of the phenylsilane-based device. Strong SAM structure–OLED response correlations are again observed, with the quantum efficiency ordering reflecting better recombination balance for the superior hole injection SAMs. The light output of the **TPD-Si₄**-based OLED is ~ 1.5 to 3 times brighter than that of **TPD-Si₂** ($\sim 50\,000$ cd/m²), **TAA-Si₁** ($\sim 45\,000$ cd/m²), and **TAA-Si₃** ($\sim 23\,000$ cd/m²) at identical bias.

Cyclic voltammetry of the SAMs on ITO (TBAHFP/CH₃CN) reveals $E_{\text{ox}}/E_{\text{red}}$ peak separations increasing in the order 331 mV (**TPD-Si₄**) < 345 mV (**TPD-Si₂**) < 382 mV (**TAA-Si₁**) < 466 mV (**TAA-Si₃**). Such data can be used to estimate interfacial electron-transfer rates for strongly absorbed redox-active sites¹⁶ and also reflect absorbate structural inhomogeneity, interactions, and electrode-redox center spacings.¹⁷ All other factors being equal, larger peak separations qualitatively correlate with slower interfacial electron transfer.^{16,18} Interestingly, this electrochemical index of heterogeneous charge injection and transport efficiency correlates closely with the solid-state hole-only device injection and transport capacity: **TPD-Si₄** > **TPD-Si₂** > **TAA-Si₁** > **TAA-Si₃** (Figure 1). The structural basis for these variations is likely associated with different SAM reorganization energies¹⁹ and different triarylamine cores having different E° values.²⁰ Additionally, the distance from the triarylamine cores to the ITO surface varies as a function of molecule geometry and linker density. **TAA-Si₃** and **TPD-Si₄** have three or four silyl linkers, respectively, while **TAA-Si₁** and **TPD-Si₂** have one or two, respectively. In principle, the former two should predominantly lie “flat” on the ITO surface, minimizing the triarylamine–anode distance, while the latter two should “stand up”, leading to different charge injection and transport characteristics.²¹ The XRR-derived SAM thickness and roughness data, combined with molecular modeling, show that **TAA-Si₃** in fact anchors largely via one linker rather than three, similar to situations

seen previously,²² while **TPD-Si₄** adopts both “flat” and “upright” orientations, yielding a rough surface. This can be correlated with the greater charge transport capacity due to the smaller $\text{NAr}_3\text{–ITO}$ anode spacing. Finally, differing intermolecular interactions between triarylamine cores likely arise from the differing molecular shapes and linker densities and should also affect interfacial charge injection and transport.^{16,17}

In conclusion, we present evidence for significant OLED anode–organic interfacial molecular structure effects on hole injection and EL properties and show that these correlate with heterogeneous electron-transfer characteristics. Chemically tuning the interface structure represents an effective approach to studying nanoscale injection layers and yields OLEDs with high brightness ($\sim 70\,000$ cd/m²), low turn-on voltages (~ 4 V), and high current efficiencies (~ 8 cd/A).

Acknowledgment. We thank USDC and NSF through the Northwestern MRSEC (DMR-0076097) for support. We thank Prof. N. Armstrong and Dr. P. Lee (University of Arizona) for UPS measurements, and Dr. B. Scott and Mr. J. Li for helpful discussions.

Supporting Information Available: Synthesis of silane reagents, SAM characterization, and device fabrication (PDF). This material is available free of charge via the Internet at <http://pubs.acs.org>.

References

- (1) For recent reviews, see: (a) Shim, H. K.; Jin, J. I. *Polym. Photonics Appl.* **2002**, *158*, 193. (b) Mitschke, U.; Bauerle, P. *J. Mater. Chem.* **2000**, *10*, 1471.
- (2) (a) Malinsky, J. E.; Veinot, J. C. G.; Jabbour, G. E.; Shaheen, S. E.; Anderson, J. D.; Lee, P.; Richter, A. G.; Burin, A. L.; Ratner, M. A.; Marks, T. J.; Armstrong, N. R.; Kippelen, B.; Dutta, P.; Peyghambarian, N. *Chem. Mater.* **2001**, *14*, 3054. (b) Shen, Y.; Jacobs, D. B.; Malliaras, G. G.; Koley, G.; Spencer, M. G.; Ioannidis, A. *Adv. Mater.* **2001**, *13*, 1234. (c) Appleyard, S. F. J.; Day, S. R.; Pickford, R. D.; Willis, M. R. *J. Mater. Chem.* **2000**, *10*, 169.
- (3) Ganzorig, C.; Kwak, K. J.; Yagi, K.; Fujihira, M. *Appl. Phys. Lett.* **2001**, *79*, 272.
- (4) (a) Cui, J.; Huang, Q.; Veinot, J. C. G.; Yan, H.; Wang, Q.; Hutchison, G. R.; Richter, A. G.; Evmenenko, G.; Dutta, P.; Marks, T. J. *Langmuir* **2002**, *18*, 9958. (b) Yu, W.; Pei, J.; Cao, Y.; Huang, W. *J. Appl. Phys.* **2001**, *89*, 2343.
- (5) Kim, J. S.; Ho, P. K. H.; Murphy, C. E.; Baynes, N.; Friend, R. H. *Adv. Mater.* **2002**, *14*, 206.
- (6) Huang, L. S.; Tang, C. W.; Mason, M. G. *Appl. Phys. Lett.* **1997**, *70*, 152.
- (7) Tutis, E.; Bussac, M. N.; Zuppiroli, L. *Appl. Phys. Lett.* **1999**, *75*, 3880.
- (8) Li, F.; Tang, H.; Andereg, J.; Shinar, J. *Appl. Phys. Lett.* **1997**, *70*, 1233.
- (9) Cui, J.; Huang, Q.; Wang, Q.; Marks, T. J. *Langmuir* **2001**, *17*, 2051.
- (10) See Supporting Information for details.
- (11) Crone, B. K.; Campbell, I. H.; Davids, P. S.; Smith, D. L. *Appl. Phys. Lett.* **1998**, *73*, 3162.
- (12) Ioannidis, A.; Forsythe, E.; Gao, Y. L.; Wu, M. W.; Conwell, E. M. *Appl. Phys. Lett.* **1998**, *72*, 3038.
- (13) Yang, S.; Wang, Z.; Xu, Z.; Hou, Y.; Xu, X. *Chem. Phys.* **2001**, *274*, 267.
- (14) Kawabe, Y.; Jabbour, G. E.; Shaheen, S. E.; Kippelen, B.; Peyghambarian, N. *Appl. Phys. Lett.* **1997**, *71*, 1290.
- (15) Huang, Q. L.; Cui, J.; Veinot, J. G. C.; Yan, H.; Marks, T. J. *Appl. Phys. Lett.* **2003**, *82*, 331.
- (16) (a) Finklea, H. O.; Liu, L.; Ravenscroft, M. S.; Punturi, S. J. *Phys. Chem.* **1996**, *100*, 18852. (b) Weber, K.; Creager, S. E. *Anal. Chem.* **1994**, *66*, 3164.
- (17) (a) Zhang, W. W.; Ren, X. M.; Li, H. F.; Lu, C. S.; Hu, C. J.; Zhu, H. Z.; Meng, Q. J. *J. Colloid Interface Sci.* **2002**, *255*, 150. (b) Nielsen, M.; Larsen, N. B.; Gothelf, K. V. *Langmuir* **2002**, *18*, 2795.
- (18) Finklea, H. O.; Hanshaw, D. D. *J. Am. Chem. Soc.* **1992**, *114*, 3173.
- (19) Murray, R. W. In *Molecular Design of Electrode Surfaces*; Murray, R. W., Ed.; Techniques of Chemistry; Wiley: New York, 1992; Vol. 22, pp 1–158.
- (20) Faber, R.; Mielke, G. F.; Rapta, P.; Stasko, A.; Nuyken, O. *Collect. Czech. Chem. Commun.* **2000**, *65*, 1403. (Core structure E° (V vs SCE) = 0.72, 0.96 (TPD); 1.02 (TAA).)
- (21) Smalley, J. F.; Feldberg, S. W.; Chidsey, C. E. D.; Linford, M. R.; Newton, M. D.; Liu, Y. P. *J. Phys. Chem.* **1995**, *99*, 13141.
- (22) Li, Z. Y.; Lieberman, M.; Hill, W. *Langmuir* **2001**, *17*, 4887.

JA037174B